Investigation of the ionospheric absorption response to flare events during the solar cycle 23 as seen by European and South African ionosondes

Veronika Barta[1], Gabriella Sátori[1], Kitti Alexandra Berényi[2, 1], Árpád Kis[1], Earle Williams[3]

[1] Geodetic and Geophysical institute, Research Centre for Astronomy and Earth Sciences, Sopron, Hungary
[2] Eötvös Loránd University, Budapest, Hungary
[3] Parsons Laboratory, Massachusetts Institute of Technology, Cambridge, USA

Correspondence to: Veronika Barta (bartav@ggki.hu)

Abstract. We have investigated the solar flare effects on ionospheric absorption with the systematic analysis of ionograms measured at mid- and low-latitude ionosonde stations under different solar zenith angles. The lowest recorded ionosonde echo, the minimum frequency (fmin, a qualitative proxy for the ''nondeviative'' radio wave absorption occurring in the D-layer), and the dfmin parameter (difference between the value of the fmin and the mean fmin for reference days) have been considered. Data was provided by meridionally distributed ionosonde stations in Europe and South Africa during eight X and M class solar flares in solar cycle 23. Total and partial radio fade-out was experienced at every ionospheric stations during intense solar flares (> M6). The duration of the total radio fade-out varied between 15 and 150 min and it was highly dependent on the solar zenith angle of the ionospheric stations. Furthermore, a solar zenith angle-dependent enhancement of the fmin (2-9 MHz) and dfmin (1-8 MHz) parameters was observed at almost every stations. The fmin and dfmin parameters show an increasing trend with the enhancement of the X-ray flux. Based on our results, the dfmin parameter is a good qualitative measure for the relative variation of the "nondeviative" absorption especially in the case of the less intense solar flares which do not cause total radio fade-out in the ionosphere (class < M6).

1. Introduction

The most intense external impact on the ionosphere from above is related to solar flares. These events are giant explosions on the surface of the Sun that suddenly release large amounts of electromagnetic energy at a broad range of wavelengths, particularly in the bands of X-radiation and extreme ultraviolet (EUV), for a very short duration (~30 minute to ~1 hour, Tsurutani et al., 2009). Solar flares are classified as large (X), medium-size (M) and small (C) according to their peak flux (in watts per square meter, Wm^{-2}, $M \sim 10^{-5} – 10^{-4}$ Wm^{-2}, $X > 10^{-4}$ Wm^{-2}) of 0.1 to 0.8 nm X-rays near Earth, as measured on the GOES spacecraft. During solar flares, the suddenly increased radiation causes extra ionization of the neutral components in the sunlit hemisphere of the Earth's atmosphere over short time intervals (few minutes to 1 hour (Rishbeth and Garriot, 1969; Tsurutani et al., 2009; Zolesi and Cander, 2014)). While hard X-rays (< 1 nm) penetrate deeply into the ionosphere and

could cause enhanced ionization in the D region during solar flares (Brasseur and Solomon, 1986; Rees, 1989; Hargreaves, 1992), the less energetic soft X-ray (1-10 nm) and far UV flux (80-102.6 nm) rather enhances the ionization in the E region (Rishbeth and Garriot, 1969). In addition to electromagnetic radiation, solar flares are also accompanied by energetic particles (protons and electrons) with energies from some tens of keV to some hundreds of MeV. They reach the Earth's atmosphere
5   between a half hour and a few hours later, and cause impact ionization (Rishbeth and Garriot, 1969; Bothmer and Daglis, 2007; Tsurutani et al., 2009). The approximate peak electron energy of a few keV causes the largest ionization in the lower E region while during the so-called solar proton events (SPE) high energy protons (up to more than 100 MeV) cause ionization much deeper, namely in the D region (Reid, 1986; Rees, 1989; Bothmer and Daglis, 2007).

10   The significant enhancement of the electron density as a result of solar flares can create increased attenuation of electromagnetic waves propagating through the ionosphere. The physical background of the ionospheric radio wave absorption mechanism is that the electrons accelerated by the electric field of the propagating radio waves collide with the atmospheric constituents. The absorbed energy of the electrons would reradiate without the presence of the neutral atmosphere. However, the electrons lose their energy due to the collisions with neutral particles which cause reduction of their reemitted signal. Since
15   the atmospheric density, the collision frequency and the recombination rate also changes with altitude, the efficiency of the radio wave absorption in the ionosphere strongly varies with altitude. The electron collision frequency is high in the D region $(2\times10^6 \text{ s}^{-1})$ and the HF radio waves below 10 MHz can be strongly attenuated there (Zolesi and Cander, 2014). Therefore, total radio fade-out lasting for tens of minutes or hours can be caused by the enhancement of electron density induced by increased electromagnetic radiation or energetic particles.

          The loss of HF communication as a result of the enhanced absorption affects navigation systems, especially in commercial aircraft operations. Therefore, describing, modelling and monitoring of the ionospheric absorption is an important issue from a practical point of view as well. The process of ionospheric absorption has been described more extensively by Davies (1990) and Sauer and Wilkinson (2008). Based on these studies the Space Weather Prediction Center (SWPC) has
25   developed a model (D-Region Absorption Prediction, D-RAP2, https://www.swpc.noaa.gov/products/d-region-absorption-predictions-d-rap) to predict the ionospheric absorption in the D-region. The product provides graphical information about High Frequency (HF) radio propagation conditions around the globe. According to the model the Highest Affected Frequency (HAF) is largest at the sub-solar point and it decreases with increasing solar zenith angle, χ (the frequencies taper off from the maximum as $(\cos\chi)^{0.75}$).

30

          Enhanced X-ray fluxes during solar flares are known to cause increased ionization in the Earth's lower ionosphere (mainly in the D region). Sahai et al. (2006) have studied the 28 October 2003 solar flare event over the Brazilian sector using ionosonde data and detected a lack of echoes in the ionograms for a 1 h period during the flare onset. They suggested that the reason for complete or partial radio signal fade-out could be intense absorption. The minimum frequency of reflection in radio

soundings by ionosondes (fmin) depends on the absorption within the D region. Sharma et al. (2010) reported on a connection between the solar flares and enhancement of fmin (> 100 %) in the ionosphere. Solar flare effects on the equatorial and low-latitude ionosphere have been described by Sripathi et al 2013. They observed the lack of ionospheric traces in the ionograms during an X class solar flare and a strong blanketing type Es layer before and after the flare event. The total radio fade-out in the ionograms was observed simultaneously with an amplified signal amplitude in ground based VLF records. They suggested that the reason of the amplified VLF signals could be enhanced D region ionization due to solar flare which could also cause the increased absorption of HF radio waves observed in the ionograms. Partial radio fade-out and a blanketing type sporadic E layer were also detected in ionograms measured close to the equator in the Brazilian sector (Denardini et al. 2016). They determined a 42-146 % enhancement in the electron density of the E-layer after X-class solar flares with the observation of peaks in the fbEs parameter. The attenuation of radio waves (below 5–8 MHz) caused by ionospheric absorption occurred some minutes before the abnormal changes in the E region electron density and can be attributed to the additional X-ray ionization due to solar flares. Total radio blackout for about 70 min and increased values of the fmin parameter inferred from ionograms registered at two ionosonde stations in the equatorial region have been reported by Nogueira et al. (2015). The onset and recovery of the flare effect were observed with a consistent time difference at the two stations. Nogueira et al. (2015) stated that the reason for this time delay is the east-west separation of the observing sites. Zaalov et al. (2018) developed an empirical absorption model combining the Global Ionospheric Radio Observatory (GIRO, http://giro.uml.edu) data and ionogram modelling. More reliable and accurate evaluation of minimum frequency is possible thanks to their proposed method.

The D region electron density (N_e) response to solar flares was studied with a medium frequency (MF) radar at Kunming (25.6°N, 103.8°E) (Li et al., 2018). They found a strong and positive correlation between N_e and X-ray changes during thirteen M class flares. Based on the results the N_e changes also depended on the onset time and the duration of the flare. Moreover, the GNSS ground and satellite receivers offered further possibilities to study the solar flare effects on total electron content (TEC) in high time (~ 30 s) and spatial resolution (Afraimovich, 2000; Zhang et al., 2002; Tsurutani et al., 2005 and 2006). Nogueira et al. (2015) observed an abrupt increase of the TEC in the sunlit hemisphere due to a flare event. The plasma density perturbation seems larger and remains for longer time in the crest region of the equatorial ionization anomaly (EIA) than at the subsolar point. However, Sripathi et al (2013) demonstrated a good correlation between the TEC enhancement caused by a solar flare and solar zenith angle. This result verifies the study of Zhang and Xiao (2005) who have shown that the ΔTEC varies with solar zenith angle. Tsurutani et al. (2009) summarized the "solar flare effects" on the ionosphere, and especially on TEC in a comprehensive review paper.

The aim of the present study is to investigate the solar flare effects on ionospheric absorption at mid- and low-latitudes, taking into account the solar zenith angle with the systematic analysis of the ionospheric fmin parameter measured at different ionosonde stations. The fmin parameter represents the minimum frequency of the echo trace observed in the ionogram and it is a rough measure of the "nondeviative" absorption (e.g. Davies, 1990). Following this introduction, the exact

method and the data examined are described in section 2. We will detail the results in section 3. Finally, the results are discussed and the concluding remarks are written in section 4.

2. Method and data

We analyzed the time series of the fmin parameter inferred from ionograms during solar flares with different intensities occurring in solar cycle 23. The ionograms have been manually verified and evaluated before the analysis. The fmin parameter, representing the lowest recorded ionosonde echo, is usually considered as a qualitative measure of the so-called ''nondeviative'' radio wave absorption in the ionosphere (Risbeth and Gariott, 1969, Davies, 1990). It is regularly used to

10   investigate the absorption of the D region in the last decades (Lusignan, 1960; Oksman et al., 1981; Kokourov, 2006; Sharma et al, 2010; Schmitter et al, 2011, Sripathi et al, 2013; Nogueira et al., 2015). However, the fmin parameter also depends on the radar characteristics and the radio-noise level. In order to minimize and compensate the instrumental errors, only data measured by Lowell type digisondes (Global Ionospheric Radio Observatory (GIRO, http://giro.uml.edu) data) were used for the investigation. Furthermore, a dfmin parameter (difference between the value of the fmin and the mean fmin for reference

15   days) have also been determined for the analysis. We chose at least 10 reference days before and after the selected flares based on the X-ray radiation ($< 0.5*10^{-4}$) and proton flux [0.8-4 MeV] ($< 3*10^3$) measured by GOES satellites. The analysis has been repeated for ionospheric data recorded at meridionally distributed ionosonde stations (the selected stations with their geographical coordinates are found in Table 1.).

20   The solar zenith angle dependence of the ionospheric response has also been investigated. We determined the solar zenith angle of the ionospheric stations at the peak time of the selected flare events. Generally, the zenith angles of the observation sites were large in Europe and small in South Africa in the case of the same flare because there are no GIRO stations between these two regions. Firstly, we investigated how the duration of the total radio fade-out depended on solar zenith angle. Then the solar zenith angle dependence of the first measured value of the fmin and dfmin parameters after the

25   fade-out was considered. In the case of the X-class solar flares the radio fade-out took 1-2 hours especially at-stations with low solar zenith angle. Consequently, in the next step we compared the solar zenith angle dependence of the fmin and dfmin parameters at a certain time after the fade-out when there were measured data at most of the stations.

We chose three X-class and further five M-class flares from three active periods for the investigation. We also

30   considered in the selection that the European and South African ionosonde stations be in the sunlit hemisphere during the flares. Therefore, the variation of absorption caused by the radiation could be determined using the fmin parameter measured at these stations. The selected solar flares are listed in Table 2. The ionograms used for the analysis were derived from the Global Ionospheric Radio Observatory network (GIRO, http://giro.uml.edu) and were processed by the SAO-X program. The

data from the GOES 11 and 12 satellite used to investigate the X-ray and solar proton flux were available at the omniweb data base (https://omniweb.gsfc.nasa.gov/).

3. Results

In the present study we investigated the response of ionospheric absorption to solar flares with particular interest of the solar zenith angle dependence variation of it. We used ionograms measured at ionosonde stations under different solar zenith angle for the analysis. We calculated the solar zenith angles of the stations at the time of the peak of the 8 flares for the analysis. We examined three parameters that can be determined from ionograms: duration of the total radio fade-out, the value

10 of the fmin parameter and the value of the dfmin parameter. In the first step we analyzed how the duration of the fade-out during the flare event depended on the solar zenith angle (Sec. 3.1). Secondly the solar zenith angle dependence of the fmin and dfmin parameters measured just after the fade-out were investigated (Sec 3.2). Then we repeated the analysis for the fmin and dfmin parameters measured at a certain time after the fade-out when we again recorded them at all the stations (3.3). In the last step the impact of the intensity variation on the absorption has been considered (3.4).

Here we demonstrate in detail the ionospheric response to an intense X17-class eruption that occurred on 28 October 2003. The European and South African ionosonde stations were located in the sunlit hemisphere during this flare event. Fig.1 shows a sequence of ionograms recorded close to the equator (Ascension Island) and at mid-latitude (San Vito) from 09:00 UTC to 14:30 UTC on 28 October 2003. Ionograms measured every 15 min were available for the analysis, however we show

20 the records with 30 minute time resolution to cover the whole time interval of the flare from the start until the end of decay. The upper panel of Fig. 2 shows the X-ray variation between 06 (UTC) and 18 (UTC) recorded by GOES12 satellite. In the X-ray flux we can clearly observe the flare event that started at 09:51, reached its peak at 11:10 and ended at 11:24. The most directly observed ionospheric effect due to the X-class solar flare is the total and partial fade-out of the sounding HF waves on the ionograms (Fig. 1.). The disappearance of the traces caused by the enhanced ionospheric absorption was recorded at both

25 stations. However, the duration of the total fade-out measured at the two observation sites was different. We may notice that an increase in the fmin parameter was first detected in the ionogram at 10:00 (UTC) over Ascension Island, close to the dip equator (fmin increased to 5.4 MHz). At San Vito, located in southern Italy at mid-latitude, the effect was weaker at this time (fmin ~ 2.9 MHz). The total attenuation of the radio waves was first recorded at Ascension Island at 11:00 (UTC). In the subsequent ionograms at 11:15 UTC (not shown here) and at 11:30 the total blackout was observed at both stations which

30 coincided with the peak in the X-ray flux as it is shown at the upper panel in Fig. 2. The trace of the F region appears on the ionogram at San Vito at 12:00 (UTC), while the total radio fade-out remains at Ascension Island until 12:30 (UTC). With the decay in the X-ray flux the blackout became partial at both stations. The fmin parameter returns to its regular daily value (~ 2.3 MHz) at San Vito at 14:00. The recovery over Ascension occurs later, partial radio fade-out was still detected at 14:30. We believe that the different duration of the total radio fade-out recorded in the ionograms at the two stations can be explained by

the different solar zenith angle at the two sites. Since the degree of the radio wave absorption in the ionosphere varies with the solar zenith angle, we compared ionograms measured at stations under different solar zenith angles to research into the solar zenith angle dependence of the ionospheric response.

5   The X-ray flux changes and dfmin parameter measured at stations with different solar angles on 27 and 28 October, 2003 are shown here (Fig. 2. and 3.). We may notice in Fig. 2 that the duration of the total radio fade-out tends to show a solar zenith angle dependence. It goes from smaller to larger values at stations with larger to smaller zenith angle. Looking at the values of the dfmin parameter detected just after the fade-out at the stations on 28 October it seems that they also follow this trend. However, this relation is not as unambiguous as in the previous case. We also compared the dfmin values recorded at a

10   certain time after the total fade-out when was observed data at all of the stations. We chose 13:00 UTC on 28 October 2003 for this comparison. As seen in the upper plot the X-ray flux at 13:00 UTC was still enhanced in contrast with its values before the flare. The values of the dfmin parameter were ~ 2-3 MHz at the mid-latitude stations at 13:00 UTC while the detected record is ~ 4 MHz at Grahamstown (low-latitude) and 6 MHz at Ascension Island (close to the equator). We can conclude in this case as well that the smaller the solar zenith angle the larger the detected value of the dfmin. A similar tendency of the

15   dfmin parameter can be seen during the two M class solar flares on 27 October 2003 (Fig. 3.). We must note that these two M class solar flares did not cause total radio fade-out in the ionosphere except at Grahamstown. The echoes were not detected there between 08:00 and 10:00 UTC. However, the solar zenith angle of the station was low (21.77°) at the peak time (at 09:30) of the M5-class flare.

20   We investigated the solar zenith angle dependence of these parameters (total fade-out, fmin, dfmin) during the other five flares. The X-ray flux and dfmin changes are not detailed here in the other cases. Nevertheless, in the next sections we will show summary plots about the solar zenith angle dependence of the values. We must note here that generally the number of observations (N) is limited to say anything about statistical significance but the plots are illustrative.

25   **3.1 Duration of the fade-out**
          Total and partial radio fade-out was experienced at every ionospheric station during and after the X class solar flares (on 2001-09-24, 2005-12-05 and on 2003-10-28) and also in the case of some M class flares (e. g. on 2006-12-06). The detected time periods of the total radio fade-out were between 15 min and ~150 min. The solar zenith angle dependence of the duration of the total fade-out has been investigated during these four events. The results are shown in the Table 3. and in Fig. 4. The

30   solar zenith angle dependence of the duration of the total radio fade-out can be clearly seen on Fig. 4. especially during the X17 flare on 28 October 2003 (Fig. 4a.) and the X9 flare on 5 December, 2006 (Fig. 4b.). The duration of the fade-out tends to increase with decreasing solar zenith angle. The tendency is similar in the other two cases but is not that pronounced.

3.2 Variation of the fmin and dfmin values just after the fade-out

The solar zenith angle dependence of the fmin and dfmin values measured at the peak time of the flares or immediately after the fade-out has been analyzed in the next step. The results are shown in Table 3 and Fig's 5. and 6. Extreme increases of the fmin values (4-9 MHz) were observed at almost every stations at the time of the X-class solar flares (on 2001-09-24, 2005-12-05 and on 2003-10-28 (Fig. 5a, 5b and 5c). Furthermore, the variation of the fmin parameter was well pronounced (2-7 MHz) during the M class solar flares as well (e. g. on 28 September 2001 (Fig. 5d.) and on 06 December 2006 (Fig. 5e.)). The solar zenith angle dependence of the fmin and dfmin values can be seen in most cases. The fmin values are increasing with decreasing solar zenith angle. This increasing trend of the fmin parameter is especially pronounced on the panels Fig. 5b., Fig. 5c. and Fig. 5e in the case of the flares 2006-12-05, 2001-09-24 and 2006-12-06 respectively. The trend can be recognized in the panels 5d., 5e, 5g and 5h, although points are more scattered. However, there is no observable trend in Fig. 5a. in the case of the most intense flare of the Halloween event on 28 October, 2003. Looking at the fmin values during the flares the effect of the different flare intensities on the ionosphere can be detectable as well. The fmin values in the case of the X-class flares in Fig. 5a. (2003-10-28) and in Fig. 5c. (2001-09-24) are larger (fmin > 5 MHz) than in the case of the M class flares from the same periods (3 < fmin < 8 MHz on Fig. 5d., 5f., 5g. and 5h.). A seasonal dependence of the fmin parameter is also evident. The values are larger in September and October (3 < fmin < 11 MHz) than in December (2< fmin < 7 MHz).

The increasing trend with decreasing solar zenith angle is also detectable in the dfmin values. Moreover, the points are not that scattered in the Fig. 6e, 6f, 6g and 6h, in the case of the M class flares. Nevertheless, the increasing trend cannot be seen in Fig. 6a and 6d. during the flares that occurred at 12:43 on 27 and at 11:24 on 28 October, 2003. The lack of an increasing trend in these cases can be explained that the times of the fade-out are very different at the different ionospheric stations (see Fig. 4.). Therefore, the first fmin and dfmin values just after the fade-out were measured at different times when also the X-ray radiation of the flare was different. In order to eliminate this possible cause for variability, we analyzed the fmin and dfmin parameters at a certain time after the peak of the flares when there were detectable values at the most stations.

3.3 Variation of the fmin and dfmin parameters at a certain time after the fade-out

Table 4, Fig. 7 and 8 show the results in connection with the solar zenith angle dependence of the fmin and dfmin values measured at a certain time after the fade-out (We demonstrated on a sample previously on Fig.2 in the case of the X17 flare occurred on 28 October 2003). The exact time of the fmin and dfmin parameter's observation, considered in this analysis, are shown in the header of different cases in Table 4. and in Fig.7 and 8. The solar zenith angle dependence of the fmin and dfmin values are more conspicuous than in the previous case. The fmin values are increasing with decreasing solar zenith angle in every case, also after the most intense flare of the Halloween event on 28 October, 2003 (see Fig. 7a.). The solar zenith angle dependence seems well defined in the dfmin values. The increasing trend appears in every case, and also after the flares that occurred at 12:43 on 27 and at 11:24 on 28 October, 2003 (Fig. 8a. and 8d.). Moreover, the points in Fig. 8. are less scattered than in the case of fmin, in Fig. 7.

3.4 Comprehensive investigation of the intensity of flares and the solar zenith angle dependence

The results showed that the ionospheric response depended also on the intensity of flare (changes in the X-ray flux). The value of the dfmin variation reached 6-9 MHz during and after the X17 (2003-10-28, Fig. 6a.) and X2 (2001-09-24, Fig. 6c.) flares. Whereas the dfmin values varied between 1 and 3 MHz in the cases of the M3.3 and M 2.4 flares on 28 September, 2001 (Fig. 6g. and 6h.). Therefore, a comprehensive analysis, taking into account the solar zenith angle and the intensity together, has also been performed. The solar zenith angle and the X-ray radiation dependence of the fmin and dfmin parameters measured at the peak of the flare events or just after the fade-out are shown in Fig. 9a. and 9b. respectively. The results show that the value of the fmin and dfmin parameters depend on the intensity of the X-ray radiation, but they also depend on the solar zenith angle of the stations where they have been measured. The largest fmin (> 7 MHz) and dfmin (> 5MHz) values have been detected during the X-class solar flares (X-ray radiation > 2.61E-04 Wm^{-2}) and at the stations with low (< 40 °) solar zenith angle. Since, the exact time of the measurements were different (because of the different duration of the total radio fade-out), this analysis has been repeated for fmin and dfmin values measured at a certain time after the fade-out when the parameters were detectable at most of the stations. (The exact observation time and the detected X-ray intensity by GOES satellites at that time are shown in the header of different cases in Table 4.) The results of the analysis are shown in Fig. 10. The X-ray radiation dependence can be seen in the value of the fmin parameter in this case as well. However, it is much better defined in the case of the dfmin parameter. Larger dfmin values (> 4.5 MHz) are related to the measurements when the X-ray radiation exceeded 3.4E-05 Wm^{-2}. Moreover, the lowest fmin and dfmin values were measured when the X-ray radiation was weaker (< 1.33E-05 Wm^{-2}) and the solar zenith angle of the stations was above 35 °.

4. Discussion and conclusion

The solar flare effects on ionospheric absorption at mid- and low-latitude have been investigated with the systematic analysis of ionograms. Three periods from solar cycle 23. were selected for analysis when eight X and M class flares occurred. The solar zenith angle of the observation sites at the time of the selected flares has also been considered in the analysis.

The lowest recorded ionosonde echo, characterized by the minimum frequency (fmin), has been used as a qualitative measure of the so-called ''nondeviative'' radio wave absorption in recent decades (Lusignan, 1960; Oksman et al., 1981; Kokourov, 2006; Sharma et al, 2010; Schmitter et al, 2011). However, a systematic analysis of this parameter measured at different ionospheric stations during solar flares has not been previously investigated. To reduce the instrumental errors a dfmin parameter (the difference between the value of the fmin and the mean fmin for reference days) has also been determined for the analysis.

Total and partial radio fade-out were experienced at every ionospheric station during and after the X class solar flares (on 2001-09-24, 2003-10-28, and on 2005-12-05) and also in the case of some M class flares (e. g. on 2006-12-06). The

observed time of the absence of the echoes was between 15 min and 150 min, similar to the findings of Sahai et al. (2006) with ionosondes over the Brazilian sector on 28 October 2003. Similarly, Nogueira et al. (2015) found from a total to partial HF blackout for about 70 min in ionograms measured at the São Luís and Fortaleza equatorial stations as a result of an X2.8 solar flare. They observed a consistent time difference in the beginning and the end of the flare effect in the sequences of ionograms and they explained this phenomenon by the east-west separation of the observing sites. We investigated the beginning and the end of the total radio fade-out measured at the eastern locations as compared to the western locations. E.g. comparing the beginning and the end of the blackout at Chilton (west) with Juliusruh (east) or at Ascension Island (west) with Grahamstown (east) during the X17 flare occurring on 28 October 2003 (Fig. 2.) we cannot detect a systematic delay. Based on our results there is no detected east-west separated consistent time difference of the flare effect. Whereas, examining the duration of the total radio fade-out at the time of the same flare (28 October 2003, Fig. 2.) it seems to depend on the solar zenith angle. The smaller the zenith angle of the observation site (Grahamstown, Ascension Island) the longer the detected blackout of the HF waves. We observed a similar trend for the flares occurring on 05 December, 2006 and on 06 December, 2006 (Fig. 4.). The total radio fade-out during the time of intense solar flares (M > 5) could be understood due to absorption of radio signals by enhanced D region ionization. Previous studies reported that enhanced ionization of the D region can lower the reflection height of the VLF radio waveguide and amplify the amplitude of the propagating signals (Thomson and Clilverd, 2001; Thomson et al., 2004; Kolarski and Grubor, 2014). Sripathi et al 2013 observed lack of ionospheric traces in the ionograms simultaneously with an amplified amplitude signal of ground based VLF records during an X class solar flare. Their results suggest there could be enhanced D region ionization due to solar flare which also caused absorption of HF radio waves in the ionograms.

Extreme increases of the fmin (4-9 MHz during X class and 2-7 MHz during M class flares) and of the dfmin (4-8 MHz at the time of the X-class flares and 1-4 MHz at the time of the M class flares) values were observed at almost every stations at the time of the flare events. These enhancements of fmin during solar flares are in good agreement with the results reported by Sharma et al. (2010) and with the values measured in South America during X-class flares (Nogueira et al. 2015, Denardini et al. 2016). The analysis of the fmin and dfmin values measured at the peak time of the flares or just after the fade-out shows a solar zenith angle dependence as well. The fmin and dfmin values are increasing with decreasing solar zenith angle. However, this increasing trend is not clear in the case of the most intense (X2 and X17) solar flares when the detected durations of fade-out are very different at the various ionospheric stations. The explanation for that can be that the first fmin and dfmin values just after the fade-out were measured at different time points when also the X-ray radiation of the flare was different. Therefore, in the next step we analyzed the solar zenith angle dependence of the fmin and dfmin parameters at a certain time after the peak of the flares when there were detectable values at most stations. The solar zenith angle dependence of the fmin and dfmin parameters is more conspicuous than in the previous case. The fmin and dfmin values are increasing with decreasing solar zenith angle in every case.

Contradictory results have been reported in the literature about the solar zenith angle dependence of the ionospheric response to solar flares. Our results are in agreement with D-RAP model (https://www.swpc.noaa.gov/products/d-region-absorption-predictions-d-rap/) on the dependence of solar zenith angle. This model was developed based on the theoretical descriptions of the ionospheric absorption by Davies (1990) and Sauer and Wilkinson (2008). According to the model the

5   Highest Affected Frequency (HAF) is largest at the sub-solar point and it decreases with increasing solar zenith angle. Moreover, Zhang and Xiao (2005) and Sripathi et al. (2013) have demonstrated a good correlation between the TEC enhancement caused by solar flares and the solar zenith angle, too. However, Li et al. (2018) concluded that there is no strong relationship between the N_e variation of the D region and the solar zenith angle. Furthermore, Nogueira et al. (2015) demonstrated an abrupt increase of the TEC. The observed anomaly seemed larger and remained for a longer time in the crest

10 region of the equatorial ionization anomaly (EIA) than at the subsolar point. We also observed the largest and the longest-lasting perturbation of the ionospheric absorption in the equatorial region (at Ascension Island) in most of the cases. However, our results suggest that the solar zenith angle of the observation site plays an important role. For instance, at the peak time of the X9 flare (05 December 2006) the zenith angle of the ionosonde station at Ascension Island (geomagnetic latitude: -2.31°) was 36.14° and the duration of the fade-out was 60 min, smaller than measured at Grahamstown (geomagnetic latitude: -

15 34.01°, see Table 3.). Even a larger difference was observed at the two stations during the M5-class flare at 09:27 on 27 October 2003. The solar zenith angle of Ascension Island was 47.96° at the peak time and there was no detected total radio fade-out. While at Grahamstown with a smaller solar zenith angle (21.77°) the duration of the total attenuation of HF waves was 150 min (Table 3.). Therefore, our observations confirm the results of Zhang and Xiao (2005), Sripathi et al. (2013) and the D-RAP model that the solar zenith angle plays an important role in the ionospheric response to solar flares.

According to the results of Li et al (2018) there is a strong correlation between the flare-induced N_e enhancement in the D-layer and the X-ray flux intensity of the flare. In order to study the impact of the X-ray flux on the fmin and dfmin parameters a comprehensive analysis, taking into account the solar zenith angle and the intensity of the flare together, has also been performed. The results show that the values of the fmin and dfmin parameters is highly dependent on the X-ray radiation

25 intensity, but it also depends on the solar zenith angle of the stations where it has been measured.

Based on the results, the dfmin parameter is a good qualitative measure for the relative variation of the "nondeviative" absorption especially in the case of less intense solar flares which do not cause total radio fade-out in the ionosphere (class < M6). However, further analysis of this ionosonde parameter and its comparison with other techniques to measure the

30 ionospheric absorption are necessary to confirm its use as a reliable index.

Competing interests. The authors declare that they have no conflict of interest.

Acknowledgement. The contribution of V. Barta was supported by the United States Department of State Bureau of Educational and Cultural Affairs as part of a Fulbright Visiting Scholar Program to the Massachusetts Institute of Technology, Cambridge, USA and by the GINOP-2.3.2-15-2016-00003 project. The contribution of G. Sátori was supported by the National Research, Development and Innovation Office, Hungary-NKFIH, K115836. The authors are grateful to the University of Massachusetts

5 Lowell Center for Atmospheric Research for the Digisonde data and SAO-X program for data processing. Data from the South African Ionosonde network is made available through the South African National Space Agency (SANSA), who are acknowledged for facilitating and coordinating the continued availability of data. This paper uses data from the Juliusruh Ionosonde which is owned by the Leibniz Institute of Atmospheric Physics Kuehlungsborn. The responsible Operations Manager is Jens Mielich. This paper uses ionospheric data from the USAF NEXION Digisonde network, the NEXION

10 Program Manager is Mark Leahy. The authors wish to thank the OMNIWeb data center for providing Web-accessible to the solar data of the Geostationary Operational Environmental Satellites (GOES) satellites.

References

Afraimovich, E. L.: GPS global detection of the ionospheric response to solar flares, Radio Sci., 35, 1417, doi:10.1029/2000RS002340., 2000

Brasseur G, Solomon S: Aeronomy of the Middle Atmosphere, Second Edition edn. D. Reidel Publishing Company, Dordrecht/Boston/Lancaster, 1986

Bothmer V. and Daglis, I. A., Space Weather, Physics and Effects, Springer, Springer Heidelberg New York Dordrecht London., 2007

Davies, K.: Ionospheric radio (No. 31). IET., 1990

Denardini, C. M., Resende, L. C. A., Moro, J., & Chen, S. S.: Occurrence of the blanketing sporadic E layer during the recovery phase of the October 2003 superstorm. Earth, Planets and Space, 68(1), 80., 2016

D-Region Absorption Prediction, D-RAP2 modell: https://www.swpc.noaa.gov/products/d-region-absorption-predictions-d-rap

Global Ionospheric Radio Observatory (GIRO): http://giro.uml.edu

Hargreaves J. K.: The Solar-Terrestrial Environment. Cambridge University Press, Cambridge, 1992

Kane, R. P.: Ionospheric foF2 anomalies during some intense geomagnetic storms, Ann. Geophys., 23, 2487–2499., 2005

Kokourov, V. D., Vergasova, G. V. and Kazimirovsky, E. S.: Long-term variations of ionospheric parameters as a basis for the study of the upper-atmospheric climate. Phys. and Chem. Earth, Parts A/B/C 31.1, 54-58., 2006

Kolarski, A., & Grubor, D.: Sensing the Earth's low ionosphere during solar flares using VLF signals and GOES solar X-ray data. Adv. Space Res., 53(11), 1595-1602., 2014

Li, N., Lei, J., Luan, X., Chen, J., Zhong, J., Wu, Q., Xu, Z. and Lin, L:. Responses of the D region ionosphere to solar flares revealed by MF radar measurements. J. Atmos. Sol-Terr. Phys., 2018

Lusignan, B.: Cosmic Noise Absorption Measurements at Stanford, California, and Pullman, Washington, J. Geophys. Res., V. 65, N. 12., 1960

Nogueira, P. A. B., Souza, J. R., Abdu, M. A., Paes, R. R., Sousasantos, J., Marques, M. S., ..., and Cueva, R. Y. C.: Modeling the equatorial and low-latitude ionospheric response to an intense X-class solar flare. Journal of Geophysical Research: Space Physics, 120(4), 3021-3032., 2015

Oksman, J., Wagner, C. U., Kaila, K. and Lauter, A. E.: Post-storm mid-latitude green aurora and electron precipitation, Planet. Space Sci. Vol. 29, No. 4, pp. 405-413., 1981

OMNIWeb data center: https://omniweb.gsfc.nasa.gov/

Rees M. H.: Physics and Chemistry of the Upper Atmosphere, 1st edn. Cambridge University Press, Cambridge, 1989

Reid G.C.: Solar energetic particles and their effects on the terrestrial environment. In: Sturrock P.A., Holzer T. E., Mihalas D. M., Ulrich R. D. (eds) Physics of the Sun, vol III, Astrophysics and solar-terrestrial relations. Reidel Publishing Company, Dordrecht, pp 251–278, 1986

Rishbeth, H., and Garriot, O. K., Introduction to Ionospheric Physics, Int. Geophys. Ser., Vol. 14, Academic Press, NY., 1969

Sahai, Y., Becker-Guedes, F., Fagundes, P. R., Lima, W. L. C., de Abreu, A. J., Guarnieri, F. L., Candido, C. M. N. and Pillat, V. G.: Unusual ionospheric effects observed during the intense 28 October 2003 solar flare in the Brazilian sector, Ann. Geophys., 25, 2497., 2006

5 Sauer, H. H., and Wilkinson, D. C.: Global mapping of ionospheric HF/VHF radio wave absorption due to solar energetic protons. Space Weather, 6(12)., 2008

Schmitter, E. D.: Remote sensing planetary waves in the midlatitude mesosphere using low frequency transmitter signals, Ann. Geophys., 29, 1287–1293., 2011

Sharma, S., Chandra, H., Vats, H. O., Pandya, N. Y., Jain, R.: Ionospheric modulations due to solar flares over Ahmedabad, Indian J. Radio Space, Vol. 39, pp. 296-301., 2010

10 Sripathi, S., Balachandran, N., Veenadhari, B., Singh, R., and Emperumal, K.: Response of the equatorial and low-latitude ionosphere to an intense X-class solar flare (X7/2B) as observed on 09 August 2011. Journal of Geophysical Research: Space Physics, 118(5), 2648-2659., 2013

Thomson, N. R. and Clilverd, M. A.: Solar flare induced ionospheric D-region enhancements from VLF amplitude observations, J. Atmos. Sol-Terr. Phy., 63, 1729–1737., 2001

15 Thomson, N. R., Rodger, C. J. and Dowden, R. L.: Ionosphere gives size of greatest solar flare, Geophys. Res. Lett., 31, L06803, doi:10.1029/2003GL019345., 2004

Tsurutani, B. T., Judge, D. L., Guarnieri, F. L., Gangopadhyay, P., Jones, A. R., Nuttall, J., ... and Meier, R. R.: The October 28, 2003 extreme EUV solar flare and resultant extreme ionospheric effects: Comparison to other Halloween events and the Bastille Day event. Geophys. Res. Lett., 32(3)., L03S09, doi:10.1029/2004GL021475., 2005

20 Tsurutani, B. T., Guarnieri, F. L., Fuller-Rowell, T., Mannucci, A. J., Iijima, B., Gonzalez, W. D., and Verkhoglyadova, O. P.: Extreme solar EUV flares and ICMEs and resultant extreme ionospheric effects: Comparison of the Halloween 2003 and the Bastille Day events. Radio Sci., 41(5)., doi:10.1029/2005RS003331, 2006

Tsurutani, B. T., Verkhoglyadova, O. P., Mannucci, A. J., Lakhina, G. S., Li, G., and Zank, G. P.: A brief review of "solar flare effects" on the ionosphere. Radio Sci., 44(1)., 2009

25 Zaalov, N., Moskaleva, E. V., Shekhovtsov, F. V.: Method of the HF wave absorption evaluation based on GIRO network data, Adv. Space Res., DOI: 10.1016/j.asr.2018.12.024, 2018

Zhang, D. H., Xiao, Z., Igarashi, K. and Ma G. Y.: GPS derived ionospheric total electron content response to a solar flare that occurred on 14 July 2000, Radio Sci., 37(5), 1086, doi:10.1029/2001RS002542., 2002

Zhang, D. H., and Z. Xiao: Study of ionospheric response to the 4B flare on 28 October 2003 using International GPS Service
30 network data, J. Geophys. Res., 110, A03307, 2005

Zolesi, B. and Cander, L.: Ionospheric Prediction and Forecasting, Springer Geophysics, Springer Heidelberg New York Dordrecht London, DOI 10.1007/978-3-642-38430-1., 2014

Ionospheric Station	Latitude (°)	Longitude (°)
Tromso	69.6	19.2
Juliusruh	54.6	13.4
Chilton	51.5	359.4
Pruhonice	50	14.6
Rome	41.9	12.5
San Vito	40.6	17.8
Ascension Isl.	-7.95	345.6
Madimbo	-22.39	30.88
Grahamstown	-33.3	26.5

Table 1. The selected ionosonde stations and their geographical coordinates.

Selected time period				
Date	X-ray class	Start [UTC]	Peak [UTC]	End [UTC]
2001-09-23 - 2001-09-28				
2001-09-24	X2.6	9:32	10:38	11:09
2001-09-28	M3.3	8:10	8:30	9:10
2001-09-28	M2.4	9:34	10:14	10:50
2003-10-27 - 2003-11-02				
2003-10-27	M5	9:21	9:27	9:32
2003-10-27	M6.7	12:27	12:43	12:52
2003-10-28	X17	09:51	11:10	11:24
2006-12-04 - 2006-12-08				
2006-12-05	X9.0	10:18	10:35	10:45
2006-12-06	M6.0	8:02	8:23	9:03

Table 2. List of selected flare events for this study.

X-ray class and time of the solar flare [UTC]				
Station name	Solar zenith angle [°]	Duration of fade-out [min]	fmin [MHz]	dfmin [MHz]
X17, 2003-10-28, 11:24				
Juliusruh	67.77	15	8.5	6.7
Chilton	65.15	50	10.4	7.8
Rome	55.07	75	8.5	5.8
San Vito	54.06	30	7.4	4.8
Grahamstown	26.09	150	6.7	4.2
Ascension Isl.	22.9	135	10.1	7
X9, 2006-12-05, 10:35:00				
Pruhonice	72.5	30	4.2	2.1
Rome	64.64	60	4.6	2.0
San Vito	63.05	30	4.2	2.4
Ascension Isl.	36.14	60	6.6	4.1
Grahamstown	12.29	75	6.7	3.6
Madimbo	9.63	90	6.1	3.5
X2, 2001-09-24, 10:38				
Juliusruh	55.31	45	5.3	3.8
Chilton	54.62	30	6.2	3.9
Rome	42.76	180	7.0	2.9
Grahamstown	33.69	0	10.6	8.1
Madimbo	25.05	90	8.0	5.6
M6.7, 2003-10-27, 12:43				
Juliusruh	71.41	0	4.3	3.2
Chilton	65.34	0	4.9	2.8
Rome	60.11	0	7.6	4
San Vito	61.34	0	5.1	3.4
Grahamstown	42.8	0	4.9	1.9
Ascension Isl.	4.82	15	6.7	3.1

X-ray class and time of the solar flare [UTC]				
Station name	Solar zenith angle [°]	Duration of fade-out [min]	fmin [MHz]	dfmin [MHz]
M6.0, 2006-12-06, 08:23				
Pruhonice	79	0	2.5	0.5
Rome	73.19	15	4.6	3.1
San Vito	69.98	0	3.6	1.9
Ascension Isl.	63.51	75	5.6	3.2
Grahamstown	23.49	75	6.4	3.6
Madimbo	18.16	90	6.9	4.1
M5.0, 2003-10-27, 09:27				
Juliusruh	69.56	0	4.3	3.1
Chilton	71.22	0	3.9	2.3
Rome	58.13	0	6.6	3.2
San Vito	55.41	0	5.1	3.3
Grahamstown	21.77	150	6.2	2.4
Ascension Isl.	47.96	0	7.5	4.8
M3.3, 2001-09-28, 08:30				
Chilton	68.97		3.7	1.7
Juliusruh	64.28		3.7	1.8
Rome	55.63		7.5	2.7
Grahamstown	38.25		5.4	3.0
Madimbo	27.86		6.6	3.1
M2.4, 2001-09-28, 10:14				
Chilton	57.85		3.2	0.9
Juliusruh	57.42		3.9	2.1
Rome	45.27		8.9	2.6
Grahamstown	31.25		4.8	2.4
Madimbo	21.25		6.5	2.9

Table 3. The ionosonde stations (first column) with their solar zenith angle (second column) at the time of the peak of the selected solar flares. The duration of the total radio fade-out at the station appear in the third column. The tabulated fmin (4th column) and dfmin (5th column) values were measured at the peak time of the flares or directly after the fade-out.

Intensity of X-ray rad. [Wm^{-2}], time of the measurement [UTC]					Intensity of X-ray rad. [Wm^{-2}], time of the measurement [UTC]				
Station name	Solar zenith angle [°]	Duration of fade-out [min]	fmin [MHz]	dfmin [MHz]	Station name	Solar zenith angle [°]	Duration of fade-out [min]	fmin [MHz]	dfmin [MHz]
7.89E-05, 2003-10-28, 13:30					8.22E-06, 2006-12-06, 10:00				
Juliusruh	74.68	15	2.9	1.9	Pruhonice	73.39	0	2.1	0
Chilton	67.64	50	5.5	3.7	Rome	65.89	15	2.4	0
Rome	64.41	75	6.3	1.9	San Vito	63.76	0	2.1	0.4
San Vito	66.26	45	3.8	2.6	Ascension Isl.	42.95	75	5.6	3.2
Grahamstown	50.09	150	6.7	3.6	Grahamstown	10.86	75	4.8	2.1
Ascension Isl.	10.81	135	8.1	6.6	Madimbo	2.9	90	6.9	4.1
1.33E-05, 2006-12-05, 12:00					3.39E-05, 2003-10-27, 09:30				
Pruhonice	73.87	30	2	0.1	Juliusruh	69.56	0	4.3	2.9
Rome	65.7	60	4.4	1.7	Chilton	71.22	0	3.9	1.8
San Vito	65.68	30	2.1	0.4	Rome	58.13	0	6.6	3.2
Ascension Isl.	18.53	60	6.6	4	San Vito	55.41	0	5.1	3.3
Grahamstown	27.65	75	6.7	4	Ascension Isl.	47.96	0	7.5	4.8
Madimbo	30.66	90	6.1	3.5	Grahamstown	21.77	150	Nan	Nan
6.06E-05, 2001-09-24, 11:30					3.26E-05, 2001-09-28, 08:30				
Juliusruh	55.57	45	4.4	3	Chilton	68.97	0	3.7	1.7
Chilton	52.34	30	5.9	3.4	Juliusruh	64.28	0	3.7	1.8
Rome	42.94	180	Nan	Nan	Rome	55.63	0	7.5	2.7
Grahamstown	38.2	0	5.9	3.5	Grahamstown	38.25	0	5.4	3.0
Madimbo	32.88	90	7.95	5.6	Madimbo	27.86	0	6.6	3.1
1.59E-05, 2003-10-27, 13:00					2.53E-05, 2001-09-28, 10:15				
Juliusruh	72.68	0	4.3	1.2	Chilton	57.85	0	3.2	0.9
Chilton	66.18	0	4.9	1.8	Juliusruh	57.42	0	3.9	2.1
Rome	61.83	0	7.6	0.9	Rome	45.27	0	8.9	2.6
San Vito	63.38	0	5.1	2.1	Grahamstown	31.25	0	4.8	2.4
Grahamstown	46.19	0	4.9	1.9	Madimbo	21.25	0	6.5	2.9
Ascension Isl.	6.64	15	6.7	3.1					

Table 4. The value of the X-ray radiation in Wm^{-2} and the date and exact time when the measurement occurred are shown in the header in every case. The ionosonde stations (first column) with their solar zenith angle (second column) at the time of the measurement after the peak of the flares. The duration of the total radio fade-out at the station appear in the third column. Also included are the measured fmin (4th column) and dfmin (5th column) values at the time of the measurement after the peak of the flares.
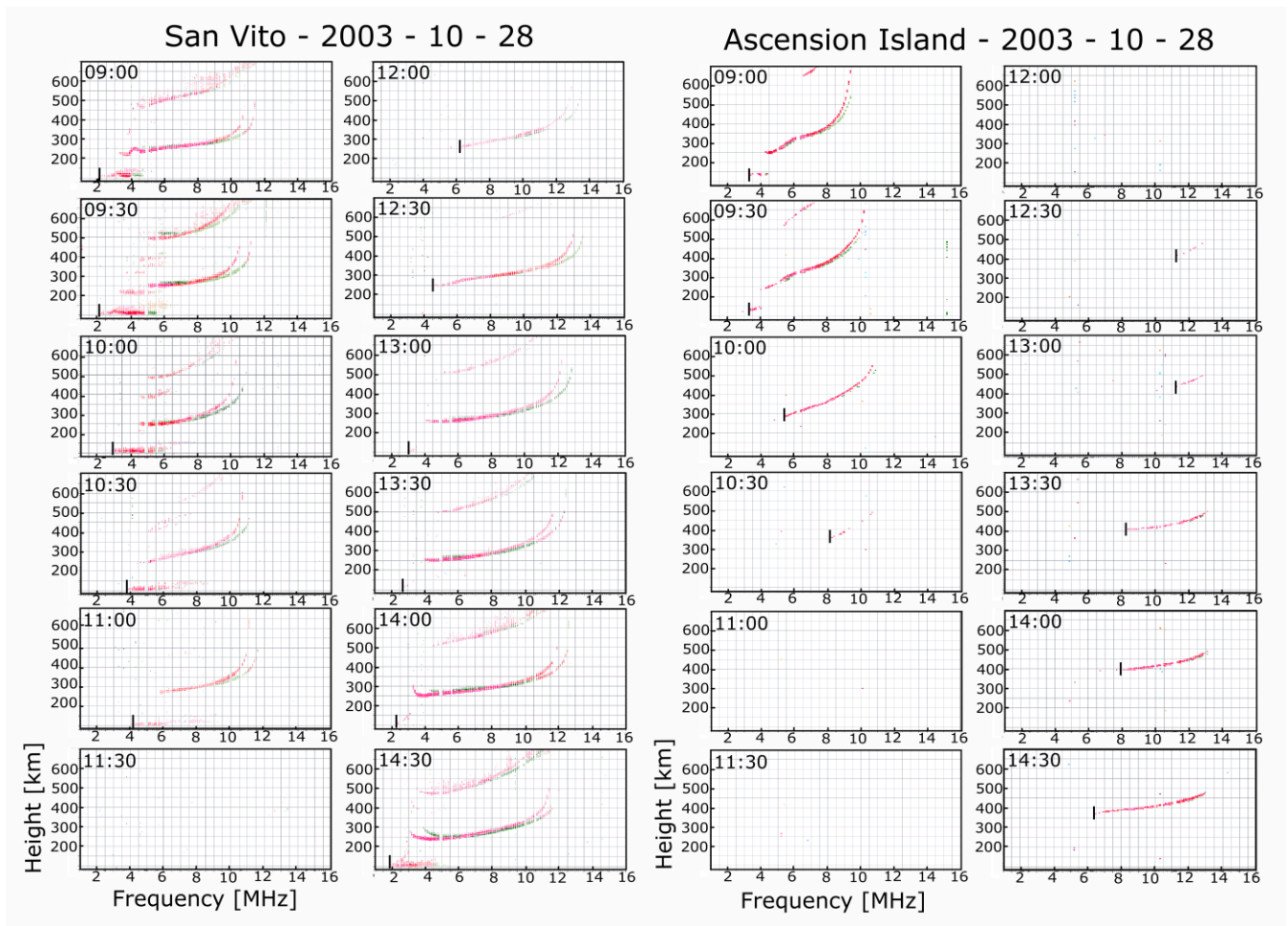
Figure 1. Sequence of ionograms at 30 min intervals recorded at San Vito (40.6, 17.8) and at Ascension Island (-7.95, 345.6) from 09:00 UTC to 14:30 UTC on 28 October 2003. This period covers the start, the peak, and decay (incomplete) of the flare X-ray flux variation. The total and partial fadeout of the sounding HF waves can be seen in the ionograms. The black vertical lines show the fmin parameter on the ionograms.
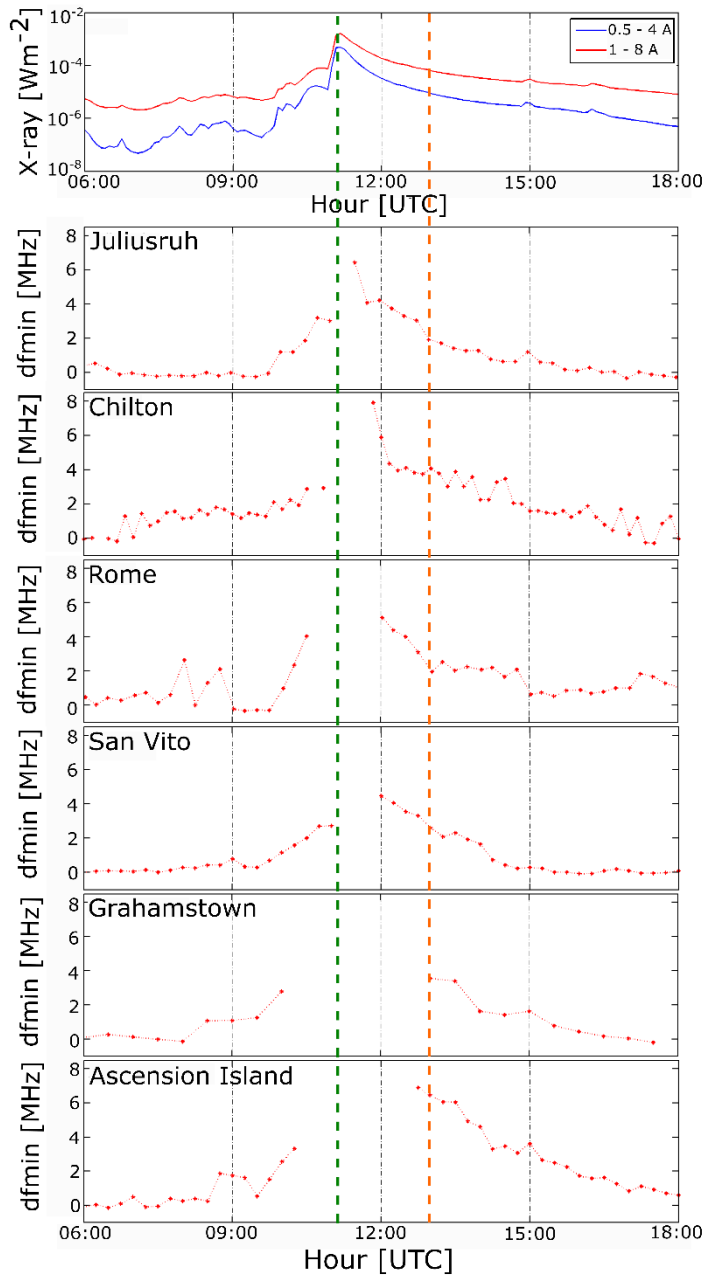
Figure 2. The variation of the X-ray flux (upper panel), the changes of the dfmin (red dots and red dashed line) parameter detected at different ionosonde stations with different zenith angle (from larger to smaller) on 28 October 2003 between 06:00 and 18:00 UTC. The vertical green dashed line shows the peak time of the X17 flare while the vertical orange dashed line shows the time used for the second comparison (13:30 UTC, in Sec. 3.3).
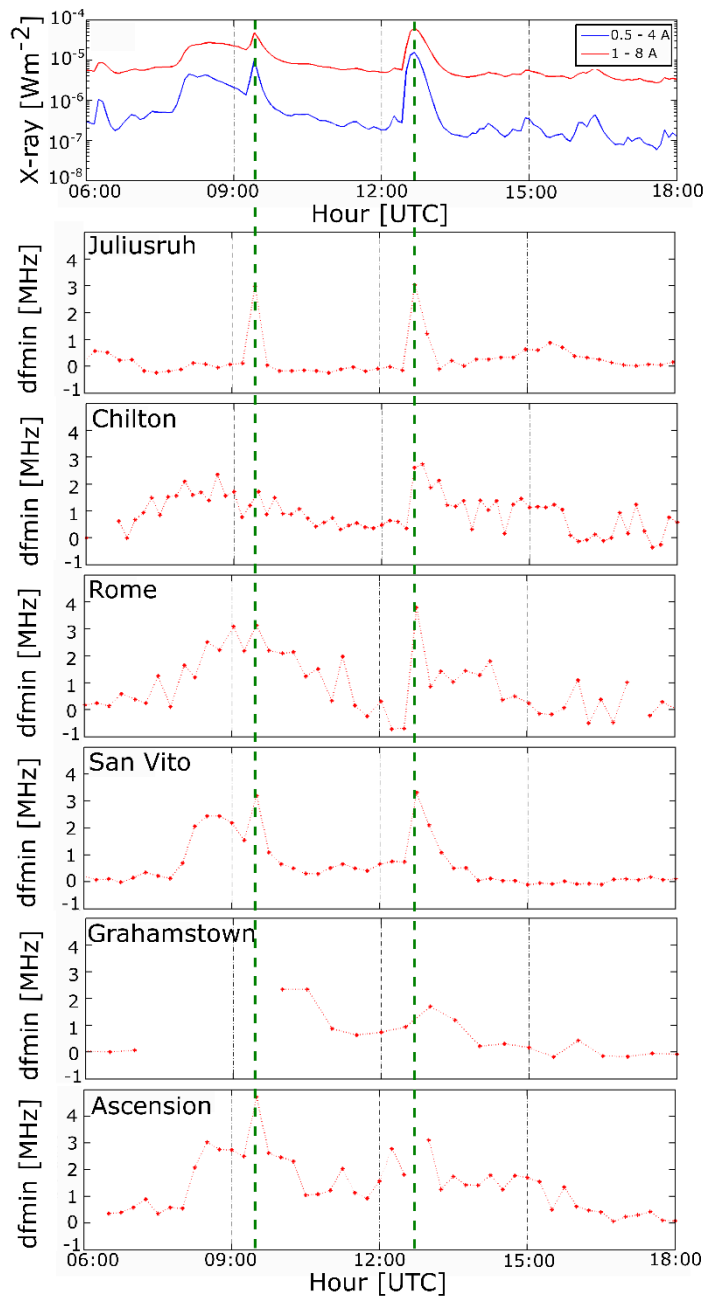
Figure 3. The variation of the X-ray (upper panel) and the changes of the dfmin (red dots and red dashed line) parameter detected at different ionospheric stations with different zenith angle (from larger to smaller) on 27, October 2003 between 06:00 and 18:00 UTC. The vertical green dashed lines show the time of the M5 (peak at 9:27 UTC) and M6.7 (peak at 12:43 UTC) flares.
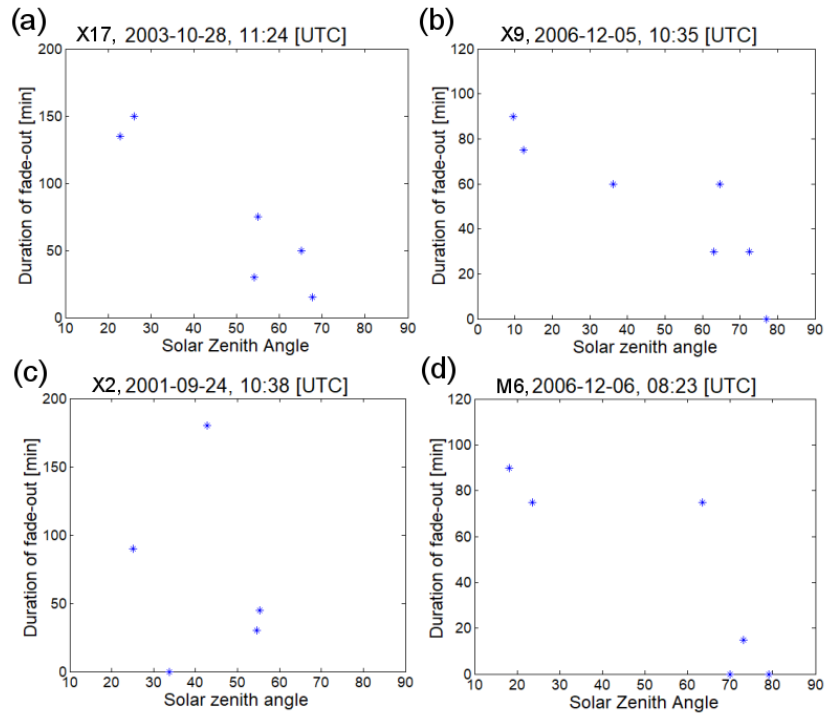
5 **Figure 4.** The solar zenith angle of the ionosonde stations at the time of the peak versus the measured duration of the total radio fade-out in the case of flare events which occurred on 28 October 2003 (a), on 5 December 2006 (b), on 24 September 2001 (c), and on 6 December 2006 (d).
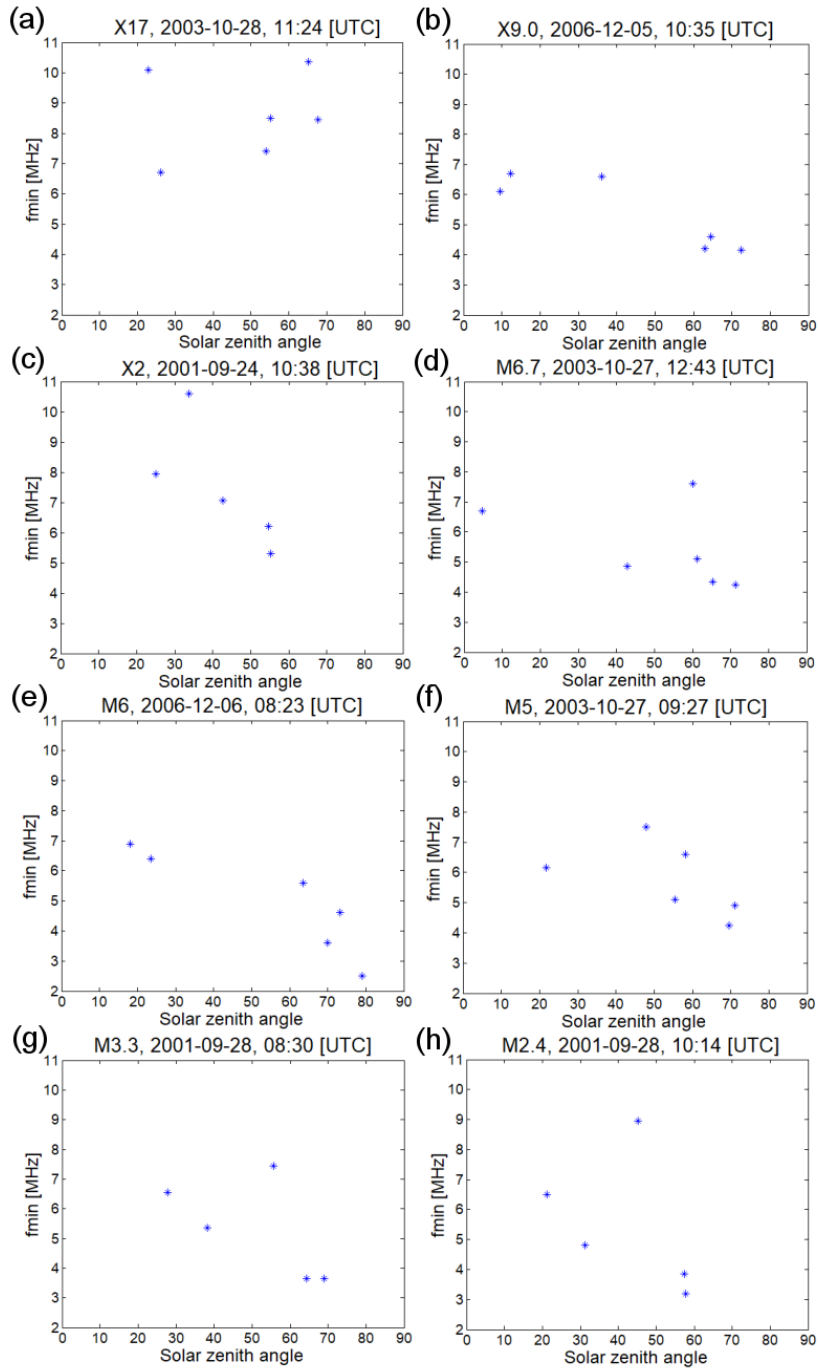
Figure 5. The solar zenith angle of the ionosonde stations at the time of the peak versus the fmin value at the peak of the flare events or after the fade-out. The X-ray class and peak time of the solar flares are seen in the title of the different panels. The results related to different flares from high to lower intensities are shown from a to h panels, respectively.
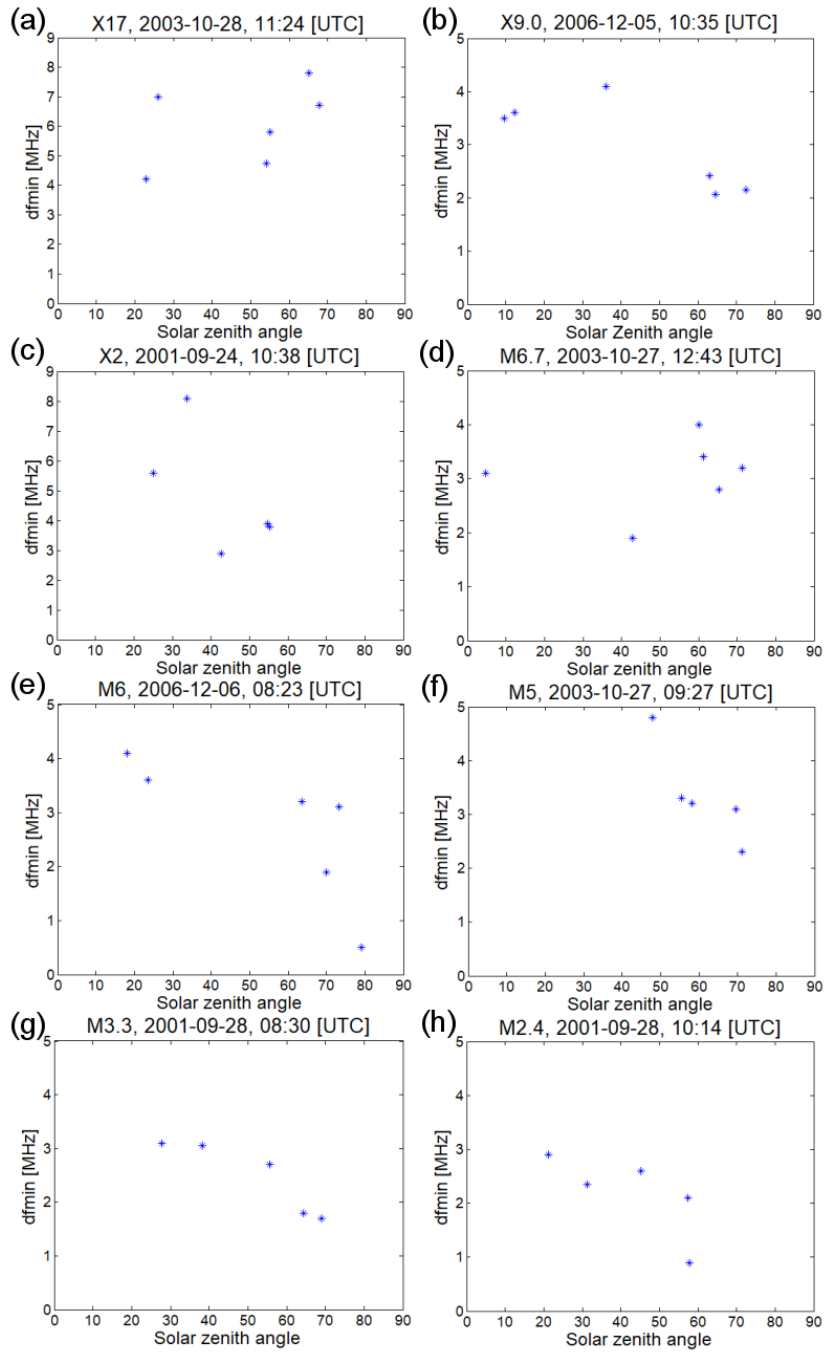
Figure 6. The solar zenith angle of the ionosonde stations at the time of the peak versus the dfmin value at the peak of the flare events or after the fade-out. The X-ray class and peak time of the solar flares are seen in the title of the different panels. The results related to different flares from high to lower intensities are shown from a to h panels, respectively.
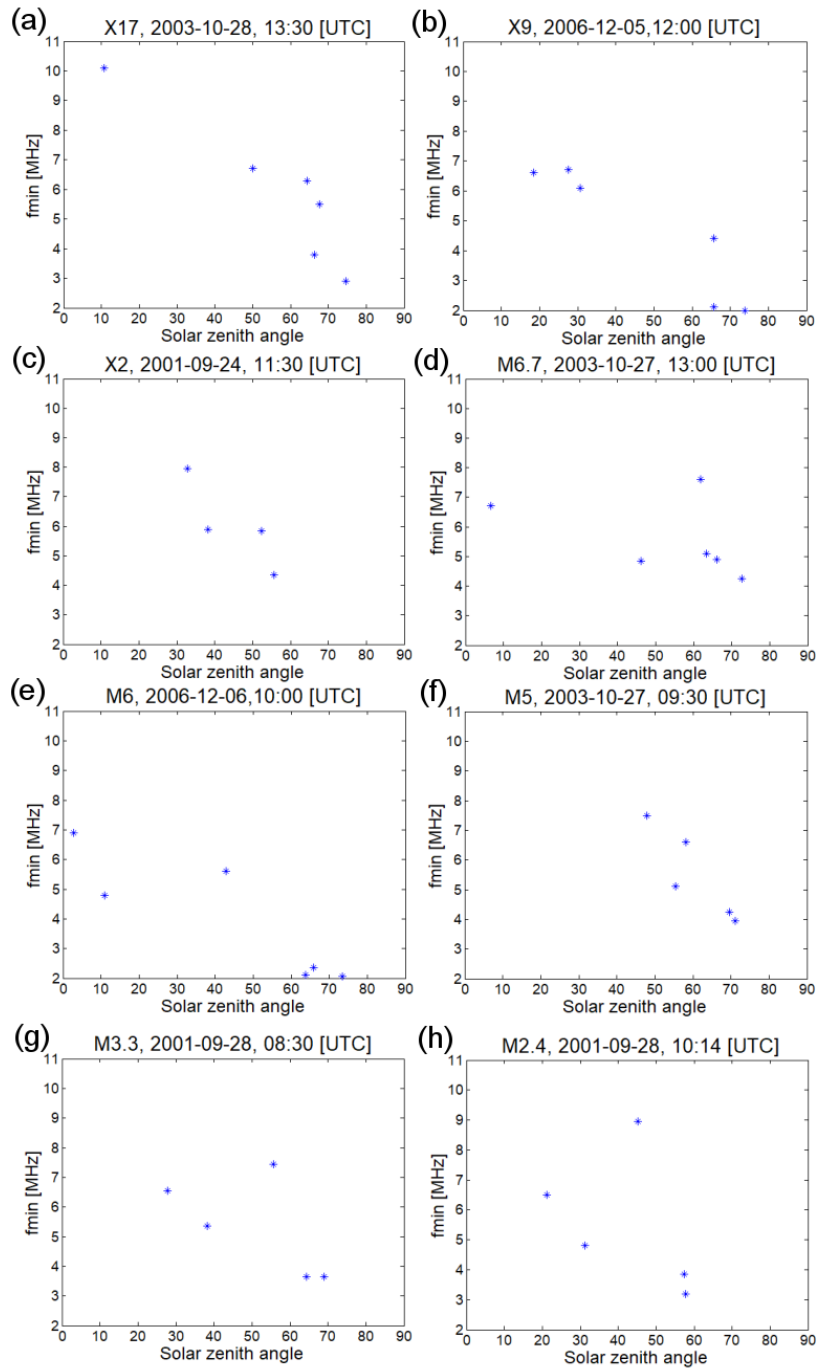
Figure 7. The solar zenith angle of the ionosonde stations at a certain time after the peak of the flares versus the fmin value at that time. The X-ray class of the flares and the time when the measurement occurred are shown in the title of the different panels. The results related to different flares from high to lower intensities are shown from a to h panels, respectively.
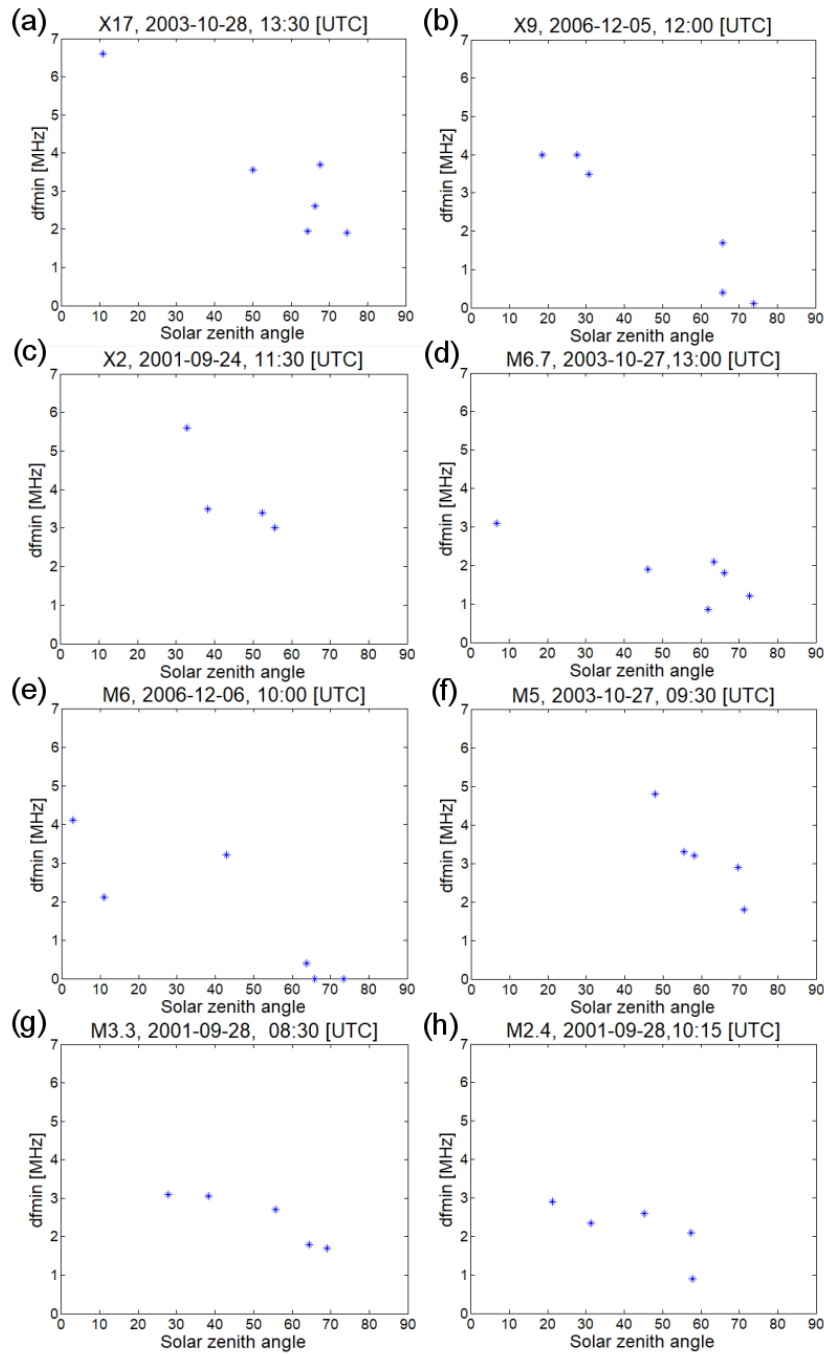
Figure 8. The solar zenith angle of the ionosonde stations at a certain time after the peak of the flares versus the dfmin value at that time. The X-ray class of the flares and the time when the measurement occurred are shown in the title of the different panels. The results related to different flares from high to lower intensities are shown from a to h panels, respectively.
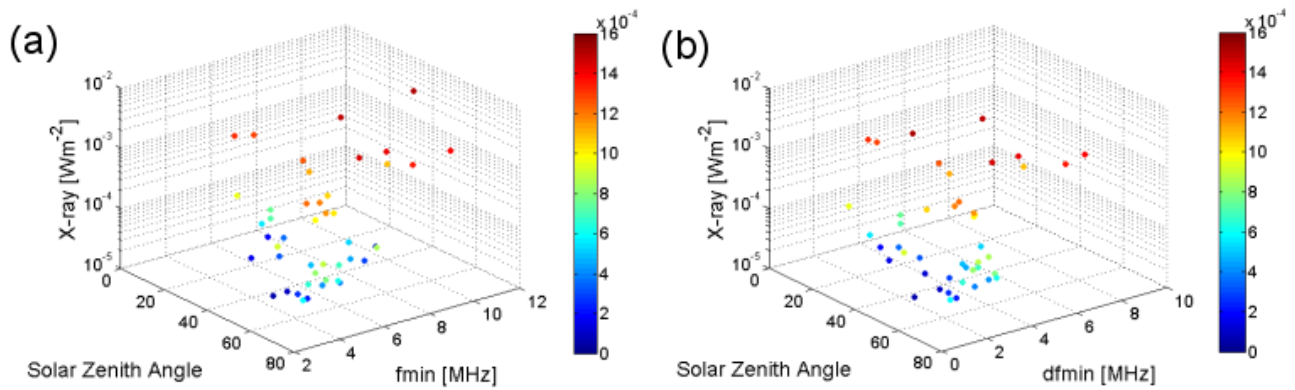
Figure 9. The solar zenith angle of the ionosonde stations at the time of the peak, the X-ray radiation at the peak and the value of the fmin (a) and dfmin (b) parameters at the peak of the flare events or after the fade-out. In order to represent the X-ray radiation dependence a colorbar has been connected to the different measurements during the flares with different intensities. The colorbar shows the X-ray radiation in Wm^{-2}.
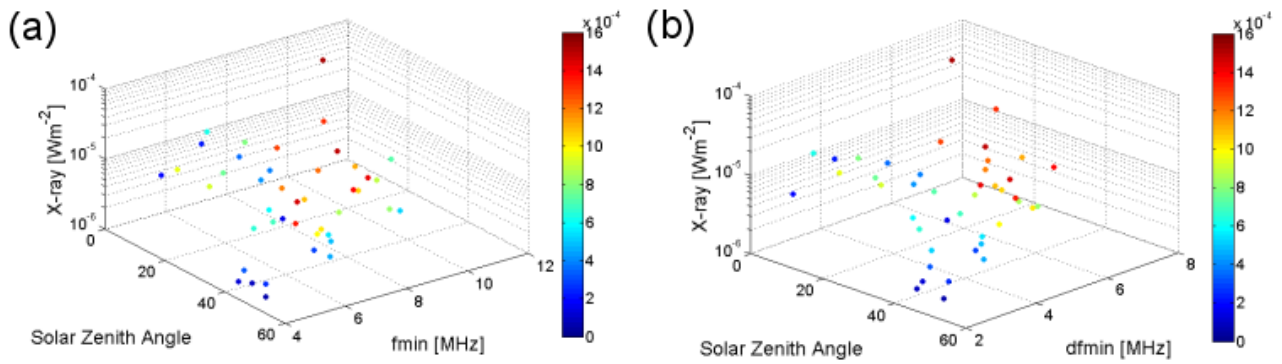
Figure 10. The solar zenith angle of the ionosonde stations at the measurement time, the X-ray radiation at the measurement time and the value of the fmin (a) and dfmin (b) parameters measured at a certain time after the peak of the flares (see text). In order to represent the X-ray radiation dependence a colorbar has been assigned to the different measurements as in Figure 11 in the previous case. The colorbar shows the X-ray radiation in Wm^{-2}.